

## Lateral diffusion coefficients of phospholipids in spherical bilayers on a solid support measured by $^2\text{H}$ -nuclear-magnetic-resonance relaxation

Thomas Köchy and Thomas M. Bayerl\*

*Technische Universität München, Physik Department E22, James-Franck-Straße, W-8046 Garching, Germany*

(Received 2 October 1992)

An alternative nuclear-magnetic-resonance (NMR) method for the measurement of the lateral diffusion coefficient  $D$  of phospholipids along the plane of a spherical bilayer on a solid support is presented.  $D$  values are determined at various temperatures for palmitoyl-oleoyl-phosphatidylcholine (POPC) bilayer on a spherical silica support of 640 nm diameter. The method is based upon the measurement of the quadrupolar transverse relaxation times obtained by the Carr-Purcell-Meiboom-Gill (CPMG) pulse sequence for a series of different pulse spacing times. It takes advantage of the fact that the CPMG sequence can progressively filter out contributions to the transverse relaxation arising from motions like lateral diffusion, which are slow on the NMR time scale. The combination of this sequence with a new membrane model system, single bilayers on a spherical support of well-defined diameter, enables the determination of  $D$ . The  $D$  values which we obtain for POPC supported bilayers [ $D = (2.1 \pm 0.7) \times 10^{-12}$  m<sup>2</sup>/s at 10°C,  $D = (4.0 \pm 0.8) \times 10^{-12}$  m<sup>2</sup>/s at 30°C, and  $D = (7.0 \pm 1.0) \times 10^{-12}$  m<sup>2</sup>/s at 50°C] are in good agreement with those obtained by other methods like fluorescence recovery after photobleaching (FRAP) and pulsed-field-gradient NMR (PFG-NMR). The discrepancies between the obtained  $D$  values and those reported recently from quasielastic neutron-scattering studies are discussed in terms of the different characteristic lengths and time scales over which the methods are sensitive. This NMR method is superior to FRAP and electron spin resonance methods since it requires no bulky labels attached to the phospholipids and it measures the average diffusion of all molecules (and not only that of the probes) in the bilayer. Moreover, the characteristic length scale of the CPMG method is significantly shorter than for FRAP or PFG-NMR. These advantages give the present method potential for the study of demixing and domain formation processes near phase transitions in model membrane systems.

PACS number(s): 87.22.Bt, 66.10.Cb, 68.35.Fx, 68.35.Ja

### INTRODUCTION

Lateral diffusion of phospholipids in membranes has been studied experimentally over the years by a variety of methods: Fluorescence recovery after photobleaching (FRAP) [1–3], excimer techniques [4], electron spin resonance (ESR) [5], NMR [6–8], and quasielastic neutron scattering (QENS) [9,10]. The lateral diffusion coefficients  $D$  of lipids determined by these methods differ by up to two orders of magnitude. As recently pointed out by Vaz and Almeida [11], the likely origin of these differences is that some methods are sensitive only to long-range diffusion (e.g., FRAP), while others (QENS) pick up contributions from extremely short-range diffusion processes.

A severe shortcoming of some of the above techniques is their reliance on labeled lipids, i.e., the diffusion coefficient measured is that of the labeled molecule and not that of the bulk lipid in the bilayer. Taking into account that the labels are often rather bulky groups (e.g., spin labels or fluorescence dyes), which can be expected to modulate the interaction of the lipid with the surrounding molecules, a discrepancy between the measured  $D$  values and the bulk lipid diffusion is quite likely. This problem is even more serious for the techniques involving bimolecular reactions (e.g., excimer methods), where phase separations due to the presence of pyrene-labeled

probes in the membrane cannot be excluded.

QENS and NMR are the only methods, which—in general—do not require any particular labeling. Even the exchange of protons by deuterons of part of a lipid, a prerequisite for  $^2\text{H}$ -NMR measurements, can be considered as a very “mild” labeling with negligible effects on the surrounding when compared to fluorescence, pyrene, or spin labeling.

Although QENS measurements on lipid membranes give the most direct information about membrane dynamics, its application is restricted due to the large substance requirements (typically 0.5–1 g per sample) and the neutron beamtime restrictions.

Hence NMR remains as the only potentially label-free method to study lateral diffusion in lipid bilayers. In the presence of a pulsed field gradient, lipid diffusion in oriented lipid multilayers has been studied as a function of hydration by spin-echo proton NMR [8]. The disadvantage of this approach is that a linear field gradient spectrometer is required and that the lipid sample (highly oriented lipid multilayers) has to be oriented in the magic angle with respect to the magnetic field in order to minimize anisotropic tensor interactions.

A recent work by Bloom and Sternin [12] paved the way for the measurement of  $D$  by broadband NMR without the need of oriented samples and field gradients. They showed that the transverse relaxation time  $T_2^*$  of

phospholipids in curved bilayers (multilamellar vesicles), obtained from two-pulse spin-echo experiments, is largely determined by motions with correlation times which are slow compared to the NMR time scale  $\tau_M$  ( $\tau_M \approx 10^{-5}$  s for  $^2\text{H-NMR}$  [13]). Lateral diffusion of phospholipids is a prime candidate for such a slow-motion mechanism characterized by  $\tau_D \gg \tau_M$ , where the diffusion correlation time  $\tau_D$  is defined by Eq. (6). In order to separate the relaxation contribution arising from slow motions, Bloom and Sternin suggested the application of the Carr-Purcell-Meiboom-Gill (CPMG) pulse sequence, giving a  $T_2^{\text{CPMG}}$  which is considerably longer than  $T_2^{\text{qe}}$  in the presence of slow motions. The CPMG pulse train for a spin-1 system ( $^2\text{H-NMR}$ ) is a  $90_x-(\tau-90_y-\tau)_N$  sequence where the  $n$ th echo ( $n=1,2,\dots,N$ ) has an amplitude given by

$$S(2n\tau) = S(0) \exp(-2n\tau/T_2^{\text{CPMG}}). \quad (1)$$

Provided that lateral diffusion is the dominating slow-motion mechanism present in a spherical lipid bilayer of radius  $R$ , the  $T_2^{\text{CPMG}}$  value can be estimated in the limit  $\tau_D \gg \tau_M$  on the basis of theoretical considerations [12,14] as follows:

$$(T_2^{\text{CPMG}})^{-1} = [(2M_{2r}D)/R^2]\tau^2 + (T_2')^{-1}. \quad (2)$$

Here  $M_{2r}$  is the residual second moment of the  $^2\text{H-NMR}$  line shape and  $(T_2')^{-1}$  is the relaxation rate due to processes having correlation times  $\tau_2'$ , which are fast on the  $^2\text{H-NMR}$  time scale ( $\tau_2' \ll \tau_M$ ).

Equation (2) opens the possibility to measure  $D$  of phospholipids by  $^2\text{H-NMR}$  without the application of external field gradients. The only requirement is a sample of spherical bilayers with known radius  $R$  (e.g., spherical vesicles with a narrow size distribution) and the membrane curvature must not exceed the limit where motional averaging effects dominate the NMR line shape (i.e.,  $\tau \ll \tau_D$ ). These requirements are fulfilled for spherical supported vesicles (SSV), which we recently suggested as an advantageous membrane model system for spectroscopic studies [15,16]. Moreover, evidence has been provided that lateral diffusion is indeed the dominating slow-motion transverse relaxation mechanism in such supported membrane systems [17].

Based on the measurement of  $T_2^{\text{CPMG}}$  for spherical supported vesicles consisting of silica beads ( $R=320$  nm), which are coated with a multilayer of 1-perdeuterio-palmitoyl-2-oleoyl-*sn*-glycero-3-phosphocholine POPC- $d_{31}$  (where POPC denotes palmitoyl-oleoyl-phosphatidylcholine) and the comparison of the data with those obtained by a random walk simulation of the CPMG spectra, we present in this work an alternative method for the determination of the lateral diffusion of lipids in model membranes. This method is demonstrated here for  $^2\text{H-NMR}$ , where deuterated lipids have to be used, but the extension of the method to  $^{31}\text{P-NMR}$  is straightforward so that no lipid labeling at all would be required.

## MATERIALS AND METHODS

### Materials

The 1-palmitoyl-2-oleoyl-*sn*-glycero-3-phosphocholine (POPC) was obtained from Avanti Polar Lipids Inc. (Alabaster, AL, USA) and used for all preparations without further purification. The spherical supports consisting of silica beads of highest purity were kindly provided by Dr. Meyer from the Degussa AG, Hanau, Germany. The radius of the beads was  $R=320 \pm 20$  nm. The size distribution was determined by electron microscopy and was found to be symmetric about the average, the beads were perfectly spherical. Scanning force microscopy measurements showed that the surface roughness of the beads is below  $3 \text{ \AA}$ .

### Methods

**Vesicle preparation:** Multilamellar vesicles (MLV) were prepared by weighing the appropriate amount of dry POPC into a test tube and adding ultrapure Millipore water to give a concentration of 25 mg/ml. After mild vortexing, the sample was incubated under nitrogen gas and gentle shaking at room temperature for 15 min.

Small unilamellar vesicles were obtained by a treatment of the MLV with a titanium rod sonifier under a nitrogen atmosphere. A temperature-controlled water bath kept the sample at room temperature during the sonification. For details see [15,18].

Spherical supported vesicles (SSV) were prepared by condensation of small unilamellar vesicles on the silica beads under controlled temperature (if not otherwise indicated  $30^\circ\text{C}$ ), according to the procedure described in [15].

Multilayers on a spherical support (spherical supported multilamellar vesicles, SSMV) were prepared by slowly drying a solution of small unilamellar vesicles containing silica beads of the desired size under a controlled vapor pressure. This was achieved by mixing beads and vesicles (prepared as described above, final concentration 50 mg POPC/ml) in a Petri dish at a POPC:bead ratio which would be sufficient to provide about 15 bilayers per bead, assuming an area of  $80 \text{ \AA}^2$  per POPC molecule. The Petri dish was then placed on a stage inside a desiccator which contained saturated NaCl solution for adjusting the vapor pressure. After closing, the desiccator was set under nitrogen gas. Then the sample was slowly dried in the closed desiccator at room temperature over a time period of two days under steady vibration of the desiccator. The vibration was adjusted to a level that ensured a continuous motion of the silica beads in the vesicle solution. The SSMV's were then filled into the NMR sample tube. Final annealing of the multilayers on the beads was achieved by incubation of SSMV's at  $60^\circ\text{C}$  for 8 h in the desiccator with saturated vapor pressure of deuterium depleted water to adjust the water content of the sample. The sample was stored at room temperature for about two days to equilibrate in the closed desiccator and plugged vapor tight afterwards. The water content of the sample was  $20 \pm 2$  wt % as measured coulometrically using a Mitsubishi CA-06 moisture meter (Mitsubishi Kasei Corp., Tokyo, Japan).

Analysis of the  $^2\text{H-NMR}$  spectrum of the sample was used to establish whether all bilayers were properly layered around the beads. Since the line shape of multilamellar vesicles without solid support is typical of an elliptical shape of the vesicles due to magnetic field orientation [18] (at the field strength used for these experiments), SSMV's must exhibit a line shape characteristic of a spherical shape. This is indeed the case since we were able to match the experimental SSMV spectra with a theoretical line shape calculated on the basis of a spherical distribution of molecular director axes (see [18] for details). A separate experiment using POPC multilayers at 20 wt % hydration (but without silica beads) showed that even such a low hydrated sample exhibits a line shape characteristic for an ellipsoidal distribution of director axes. Thus the line shape obtained for the SSMV's indicates that at least 90% of the lipids are layered around the silica beads.

### $^2\text{H-NMR}$ measurements

$^2\text{H-NMR}$  measurements were performed at 62 MHz using a Varian VXR 400 spectrometer equipped with a Varian broadband high-power probe with a 10-mm sample coil. A quadrupolar echo and a quadrupolar Carr-Purcell-Meiboom-Gill sequence  $[90_x^\circ - (\tau - 90_y^\circ - \tau)_n]$ ,  $n = 1, 2, 3, \dots, N$  sequence with a cyclops phase cycling scheme [19] were used. The number of transients was 1000 for the SSMV's and 5000 for the SSV's, respectively. A recycle delay of 0.5 s and a dwell time of 1  $\mu\text{s}$  were applied. The pulse length for a  $90^\circ$  pulse was 6  $\mu\text{s}$ .

The pulse spacing times  $\tau$  were varied between 30 and 200  $\mu\text{s}$  in the quadrupolar echo experiments and between 20 and 100  $\mu\text{s}$  in the CPMG experiments. An additional  $90_y^\circ$  refocusing pulse was applied 35  $\mu\text{s}$  after the last echo in the CPMG sequence to get rid of problems due to ring down and transmitter-receiver switching times at very short pulse spacing times  $\tau$ . This additional pulse was applied to all CPMG experiments.

### Random walk diffusion simulation of quadrupolar echo and CPMG transverse relaxation

The simulation of the  $^2\text{H-NMR}$  spectra of the supported vesicles of POPC- $d_{31}$  was done using the same numerical algorithm as described in [17]. The effect of diffusion was introduced by a random walk simulation of molecules on a spherical surface with radius  $R$ . An axially symmetric quadrupolar interaction tensor was assumed with different quadrupolar splittings  $\Delta\omega_j$  for every deuterium position in the molecule, according to the order parameter profile of POPC- $d_{31}$  bilayers. The order parameter profile was determined by a procedure of numerical deconvolution of a spectrum according to [20].

Fifty thousand molecules were distributed equally over the sphere. The surface of the sphere was divided into 50 000 angular elements  $\Delta\Theta_k$  with equal area. So a position  $\Theta = \Theta_k$  was assigned to each molecule  $k$ . At  $t = 0$  the phases of all spins were set to zero (corresponding to the time immediately following the first, infinitely short  $90_x^\circ$  pulse in a quadrupolar echo or CPMG sequence). Then diffusion was introduced by random jumps in con-

stant time intervals  $\Delta t$  (dwell time) with a jump angle  $\delta = (4D\Delta t)^{1/2}/R$  [21]. The program keeps track of the position of the molecules after the jump and of the acquired phase  $\Phi_k$  for each molecule. After  $N_d$  diffusion jumps  $\Phi_k$  is given by

$$\Phi_k(t = N_d\Delta t) = \sum_j \sum_{i=1}^{N_d} \omega_{jk}(t = i\Delta t)\Delta t, \quad (3)$$

where  $\omega_{jk}(t = i\Delta t)$  is the frequency of spin  $j$  of molecule  $k$  (corresponding to its angular position  $\Phi_k$ ) after the  $i$ th jump. At a time  $t = \tau$  the acquired phase  $\Phi_k$  is reversed by multiplication with  $-1$  (effect of an infinitely short  $90_y^\circ$  pulse). The random jumps continue and the free-induction decay (FID)  $S(t)$  forms an echo at  $t = 2\tau$  given by

$$S(t) = \sum_{k=1}^{N_{\text{tot}}} \exp[i\Phi_k(t)], \quad (4)$$

where  $N_{\text{tot}}$  is the total number of molecules on the sphere.

For the simulation of a quadrupolar echo experiment now the rest of 4096 jumps were accumulated. The spectra were obtained by Fourier transformation starting at  $t = 2\tau$ . An isotropic line broadening of 350 Hz was applied to the time domain signal, corresponding to an isotropic  $T_2'$  in Eq. (2), before Fourier transformation, as revealed from the experiments (see Results section).

For simulation of CPMG experiments the phase  $\Phi_k(t)$  was reversed by multiplication with  $-1$  at time  $t = (2n + 1)\tau$ ,  $n = 0, 1, 2, \dots, N$ . So  $S(t)$  forms echoes at times  $2n\tau$ .

### Calculation of transverse relaxation times

The average transverse relaxation time  $T_2^{\text{qe}}$  was calculated by fitting a single exponential to the decay of the spin-echo signal (FID echo) using a  $\tau$  range from 50 to 150  $\mu\text{s}$ .

The frequency-dependent relaxation time  $T_2^{\text{qe}}(\omega)$  was calculated from a series of spectra with pulse delay times  $\tau$  from 30 to 120  $\mu\text{s}$ , assuming that a single exponential decay for each frequency point in the spectrum can be calculated. The simulated spectra have been weighted before Fourier transformation with a Lorentzian line broadening of 350 Hz, corresponding to a  $T_2'$  in Eq. (2) of approximately 900  $\mu\text{s}$ , as in the CPMG experiments on POPC bilayers.

The average CPMG relaxation time  $T_2^{\text{CPMG}}(\tau)$  for the different pulse spacing times  $\tau$  was calculated using a single exponential fit to the first  $n$  FID echoes, so that  $2n\tau \approx 300 \mu\text{s}$ .

## RESULTS

Among the major advantages of the use of spherical supported vesicles for broadline NMR studies is their well-defined spherical geometry and size. This enables a direct comparison of the experimental NMR data with random walk jump diffusion simulations on a sphere with the same diameter as used in the experiment. For this work, we used spherical supported unilamellar and mul-

tilamellar vesicles (SSV's and SSMV's) with a radius of  $R = 320$  nm. The SSMV's were coated on the average with 15 bilayers of POPC- $d_{31}$ .

In a previous work, we have demonstrated that the  $^{31}\text{P}$ -NMR transverse relaxation of this system can be explained by the lateral diffusion of the phospholipids along the bilayer plane, where the curvature of the latter corresponds to that of the spherical support [17]. This result suggests that it should be possible to use NMR relaxation techniques on SSMV's for the determination of the phospholipid lateral diffusion constant  $D$ . However, the use of  $^{31}\text{P}$ -NMR has two disadvantages: it probes only one nucleus per lipid molecule and the proper phasing of the spectra is more difficult compared to spectra of spin-1 nuclei.  $^2\text{H}$ -NMR in combination with the quadrupolar echo (QE) technique can overcome these shortcomings since one can apply lipids with perdeuterated fatty acyl chains and phasing is conveniently done by adjusting the quadrature signal to zero prior to the Fourier transform.

In a first step we wish to demonstrate that the anisotropic transverse relaxation of  $^2\text{H}$ -NMR spectra of SSMV's obtained with the QE sequence (giving  $T_2^{\text{QE}}$ ) can be understood in a satisfactory way as caused by lateral diffusion of phospholipids.

In Fig. 1 we present experimental and simulated  $^2\text{H}$ -NMR quadrupolar echo spectra of SSV of POPC- $d_{31}$  at  $30^\circ\text{C}$  obtained at increasing echo times  $2\tau$ . The random walk jump diffusion simulation was performed assuming that the sole anisotropic transverse relaxation mechanism is lateral diffusion of the phospholipids along a spherical bilayer with the same diameter as the SSV's and with  $D = 5 \times 10^{-12}$  m $^2$ /s (see Materials and Methods section for details). An isotropic contribution to  $T_2^{\text{QE}}$  was assumed in the simulated spectra using a Lorentzian line broadening of 350 Hz, corresponding to a  $T_2'$  in Eq. (2) of approximately 900  $\mu\text{s}$ , as seen in the experiment. The value of  $D$  used in the simulations corresponds to values measured for diffusion in lipid bilayers by various methods [6]. A comparison shows that the simulation can indeed account for all transverse relaxation features of the experimental spectra. This becomes even more obvious in Figs. 1(c) and 1(d), where the relaxation spectra calculated from the series of experimental spectra and simulated spectra, respectively, are shown. The construction of relaxation spectra is a convenient way to visualize and to quantify anisotropic relaxation of broadline NMR spectra [22]. Both experiment and simulation give an anisotropic relaxation behavior which can be approximated for every  $^2\text{H}$  position in the molecule by

$$1/T_2^{\text{QE}} = A + B \sin^2(\theta) \cos^2(\theta), \quad (5)$$

where  $\theta$  is the angle between the molecular director axis and the magnetic field.

The excellent agreement of the  $T_2^{\text{QE}}(\omega)$  values in this representation provide evidence that the  $T_2^{\text{QE}}$  measured experimentally for SSV's and SSMV's can be explained by lateral diffusion.

A plot of the logarithm of the signal intensity at the top of the echo versus the time  $2\tau$  between the first  $90^\circ$  pulse and the echo (see Fig. 2) for the experimental data

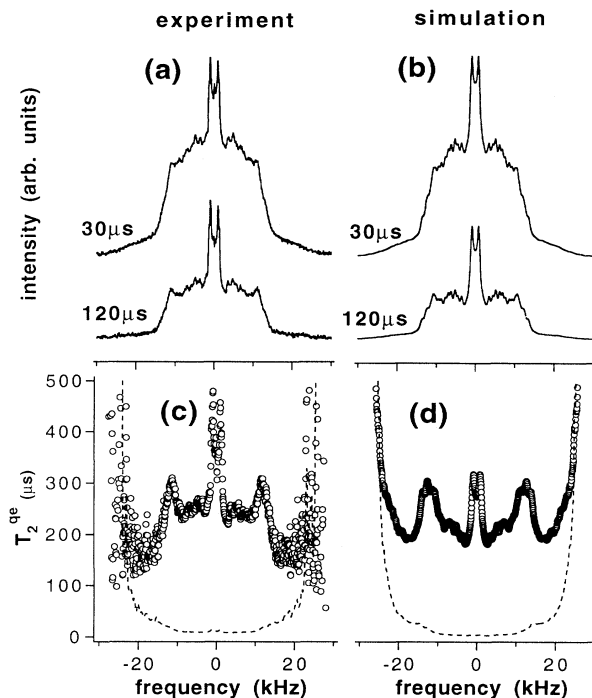


FIG. 1. (a),(b)  $^2\text{H}$ -NMR spectra of POPC- $d_{31}$  spherical supported vesicles (SSV) obtained by (a) the quadrupolar echo technique at a temperature of  $30^\circ\text{C}$  and by (b) a random walk jump diffusion simulation of the quadrupolar echo with  $D = 5 \times 10^{-12}$  m $^2$ /s as a function of the pulse spacing time  $\tau$ :  $\tau = 30$   $\mu\text{s}$  (upper spectra),  $\tau = 120$   $\mu\text{s}$  (lower spectra). (c),(d)  $^2\text{H}$ -NMR relaxation spectra calculated from the data shown in (a) and (b): (c) experimental data and (d) simulated data. The open circles represent the  $T_2^{\text{QE}}(\omega)$  values obtained for single exponential fits to each frequency point (see Materials and Methods section for details), the dashed lines show the error of these fits.

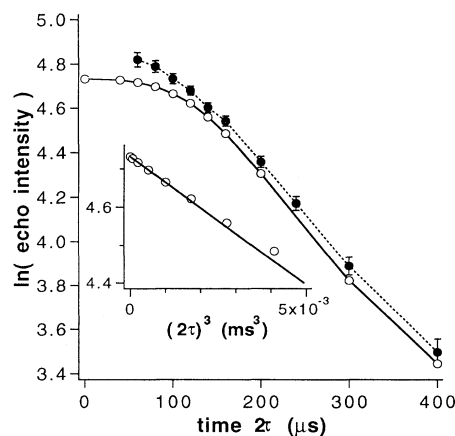


FIG. 2. Plot of the logarithm of the quadrupolar echo intensity versus time  $t = 2\tau$  for the SSV sample of POPC- $d_{31}$  obtained by simulation (open circles) and by experiment (full circles). The inset shows the logarithm of the initial decay of the simulated quadrupolar echo as a cubic function of the time.

of POPC SSV ( $R = 320$  nm) at  $30^\circ\text{C}$  and for the simulation with  $D = 5 \times 10^{-12}$  m<sup>2</sup>/s shows a nonexponential decay for the simulated echo at short times which can be described by an  $\exp(-\tau^3)$  law (inset in Fig. 2). In fact, this  $\tau^3$  decay of the echo intensity is expected from a theoretical treatment of the effect of lateral diffusion on  $T_2^{\text{qe}}$  for spherical vesicles in the limit  $\tau \ll \tau_D$  [23], where the latter is the diffusion correlation time which can be calculated from the radius of the sphere as [24]

$$\tau_D = R^2/6D. \quad (6)$$

Since this  $\tau^3$  decay dominates at very short times only (up to  $t = 2\tau \approx 150$   $\mu\text{s}$ ), it cannot be completely observed experimentally since technical limits of the spectrometer system (ringdown time of the probe and pulse length) do not permit reliable measurements over the whole short-time range. Moreover, the possible presence of adiabatic surface roughness of the bilayer has been demonstrated to straighten out the  $\tau^3$  decay [17]. At longer times, however, both experimental and simulated echo signal decay exhibit a very similar orientationally averaged  $T_2^{\text{qe}}$ :  $230 \pm 25$   $\mu\text{s}$ , for the experiment and  $220 \pm 20$   $\mu\text{s}$  for the simulation.

Thus, matching the experimental  $T_2^{\text{qe}}$  with that obtained from the exponential part of the simulation is a potential method for the determination of  $D$ . However, this is rather time consuming since it always requires a new simulation for various  $D$  values when one or several experimental parameters (e.g., temperature, SSMV size, hydration, or lipid type) are changed.

A more convenient way of measuring  $D$  which does not require simulations is the use of the quadrupolar CPMG pulse sequence [25,26]. This sequence has been applied previously on phospholipid multilamellar vesicles [12] in order to demonstrate the effect of slow motions on transverse relaxation and for the determination of the average diameter of the vesicles (assuming a value of  $D = 4 \times 10^{-12}$  m<sup>2</sup>/s).

Figure 3 shows the decay of the echo intensity for the POPC- $d_{31}$  SSMV's obtained by a CPMG experiment [Fig. 3(b)] and by a CPMG simulation ( $D = 5 \times 10^{-12}$  m<sup>2</sup>/s) [Fig. 3(a)]. The echo amplitudes obey Eq. (1) and the separation between consecutive echoes is  $2n\tau$ . The first CPMG echo corresponds to the quadrupolar echo.

As in the case of the quadrupolar echo, the CPMG simulation results agree remarkably well with the experiment. The slower decay of the simulated CPMG is due to the fact that this simulation does not consider any transverse relaxation contributions with correlation times  $\tau'_2 \ll \tau_M$ .

The nonexponential decay of the echoes shown in Fig. 3(b) is a result of the superposition of  $T_2^{\text{CPMG}}$  orientation dependencies and of different values at the positions along the perdeuterated palmitoyl chain of the POPC- $d_{31}$ .

The simulation can now be used to assign the time range over which the slope of a linear fit of  $(T_2^{\text{CPMG}})^{-1}$  versus  $\tau^2$  reflects the value of  $D$  according to Eq. (2). Figure 4(a) shows such a plot of  $(T_2^{\text{CPMG}})^{-1}$  determined from the first two "echoes" (at  $t = 0$  and  $2\tau$ ) in the CPMG simulation. The straight line is calculated from

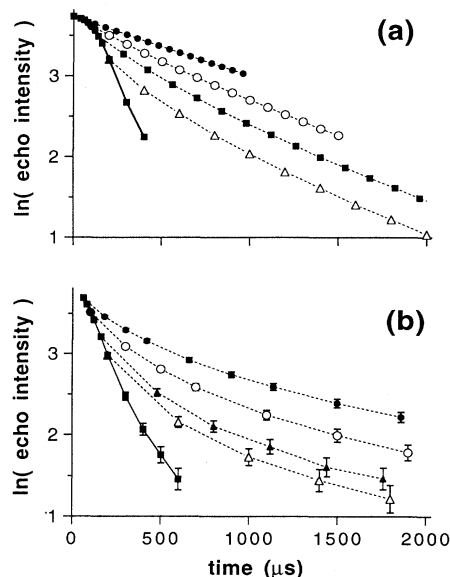


FIG. 3. Semilogarithmic plot of the echo intensity vs time  $t = 2n\tau$  (where  $n$  is the number of the echo) for different values of the pulse spacing  $\tau$  obtained by (a) CPMG simulation ( $R = 320$  nm,  $D = 5 \times 10^{-12}$  m<sup>2</sup>/s) and by (b) a quadrupolar CPMG experiment on POPC- $d_{31}$  SSMV ( $T = 30^\circ\text{C}$ ). The values of  $\tau$  were 30  $\mu\text{s}$  (full circles), 50  $\mu\text{s}$  (open circles), 70  $\mu\text{s}$  (full squares), 80  $\mu\text{s}$  (full triangles), and 100  $\mu\text{s}$  (open triangles). The solid line represents the quadrupolar echo experiment.

Eq. (2) with  $D = 5 \times 10^{-12}$  m<sup>2</sup>/s (and all other parameters) as used in this simulation. The linear extrapolation of the data to zero time intercepts the vertical axis at zero, since the simulation considers only diffusion as a transverse relaxation mechanism [i.e.,  $(T_2')^{-1} = 0$ , cf. Eq. (2)]. The deviation of the data points from the calculated line for longer values of  $\tau$  in the simulation shows that for the determination of the lateral diffusion coefficient  $D$  only the initial slope up to a pulse delay time  $\tau_{\text{max}}$  is relevant. The upper time limit  $\tau_{\text{max}}$  roughly corresponds to the time domain, where the  $\exp(-\tau^3)$  decay can be observed for the quadrupolar echo (cf. Fig. 2, inset). Thus only the first few experimental  $(T_2^{\text{CPMG}})^{-1}$  values (obtained for the shortest possible  $\tau$ 's) will be required for the determination of  $D$ .

Figure 4(b) shows a plot similar to Fig. 4(a), but for the experimentally obtained  $(T_2^{\text{CPMG}})^{-1}$  values of the SSMV sample at  $10^\circ\text{C}$  and  $30^\circ\text{C}$  in the short  $\tau$  limit. Table I lists the slope and the value of  $D$  for this sample obtained by extending the linear fit according to Eq. (2) over different numbers of data points as shown in Fig. 4(b), starting with the data point obtained for the shortest  $\tau$ . It should be noted here that the CPMG pulse sequence permits measurements down to very short pulse spacings  $\tau$  but that the lower limit is given by "spin-locking" effects, which ultimately inhibit the dephasing of the magnetization in the very-short-time limit. Up to five data points were considered for the fitting procedure; data points at longer times are not suitable for the data analysis as shown by Fig. 4(a). The results shown in

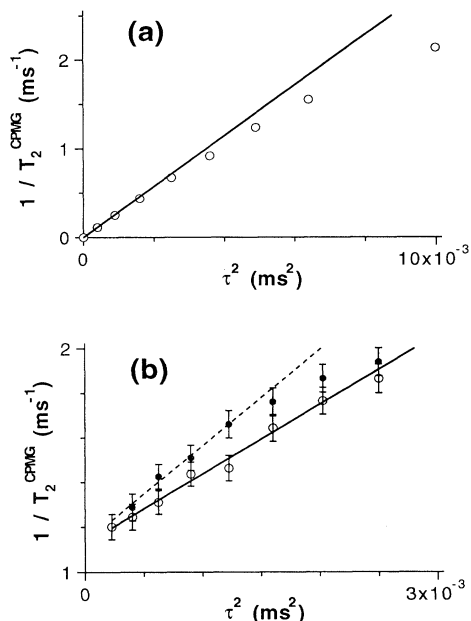


FIG. 4. (a) Plot of the simulated  $(T_2^{\text{CPMG}})^{-1}$  of POPC vesicles with a diameter of 640 nm vs  $\tau^2$  for a lateral diffusion constant  $D = 5 \times 10^{-12}$  m<sup>2</sup>/s. The straight line has a slope which corresponds to this value of  $D$  according to Eq. (2). (b) Plot of the inverse of the experimental  $(T_2^{\text{CPMG}})^{-1}$  of POPC vesicles 640 nm in diameter vs  $\tau^2$  at a temperature of 10°C (open circles) and 30°C (full circles). The full line represents a linear fit over the first six data points of the 10°C experiment, the dashed line represents a linear fit over the first four data points in the 30°C experiment, giving a slope and a lateral diffusion coefficient as listed in Table I.

Table I can give a measure of the reliability of the method for the determination of  $D$ . The variation of the  $D$  values around the average is  $\pm 0.5 \times 10^{-12}$  m<sup>2</sup>/s. Considering additionally the error of the measurement due to the size distribution of the silica beads and that of the second moment calculation we end up with a total error of  $D$  of  $\pm 0.7 \times 10^{-12}$  m<sup>2</sup>/s. Hence we obtain  $D = (2.1 \pm 0.7) \times 10^{-12}$  m<sup>2</sup>/s for POPC at 10°C. For the linear fit of this data [straight full line in Fig. 4(b)] only the first six data points were considered. The slope of the line gives  $D = 2.1 \times 10^{-12}$  m<sup>2</sup>/s and the intercept with the vertical axis yields  $T_2' = (890 \pm 70)$   $\mu$ s. Similar measure-

ments were performed at higher temperatures and yielded  $D = (4.0 \pm 0.8) \times 10^{-12}$  m<sup>2</sup>/s at 30°C and  $D = (7 \pm 1) \times 10^{-12}$  m<sup>2</sup>/s at 50°C.

## DISCUSSION

There are two aims of this paper: One is to demonstrate that lateral diffusion of phospholipid molecules in curved membranes is the dominating  $T_2^{\text{qe}}$  relaxation mechanism and the other is to present a reliable method for the determination of  $D$  from the transverse relaxation behavior of a spherical supported membrane.

In general, there are three independent mechanisms conceivable in fluid lipid bilayers which can modulate the direction of the molecular director axis (in our case corresponding to the long axis of the phospholipid molecules) during the time  $\tau$  of the quadrupolar echo experiment (slow motion regime) and thus contribute to  $T_2^{\text{qe}}$ . These are (1) lateral diffusion of the phospholipids along the bilayer surface, (2) thermally excited collective surface undulations of the bilayer, and (3) collective director fluctuations. For all three mechanisms it has been shown theoretically [12,27] and for (3) also experimentally [28,29] that they give rise to an anisotropic  $T_2^{\text{qe}}$  as described by Eq. (5). The possible contributions of these mechanisms to transverse relaxation in spherical supported bilayers has been discussed in detail previously [17]. However, only lateral diffusion can be expected to give rise to an  $\exp(-\tau^3)$  dependence of the quadrupolar echo signal at short  $\tau$  under our experimental conditions. This behavior is most clearly observed for the simulated quadrupolar echo experiments (Fig. 2) where no technical limits regarding the fidelity and the duration of the pulses exist. The experimental data [Figs. 1(c) and 1(d)] indicate that this decay is indeed a salient feature of spherical membranes. Moreover, the experimentally obtained value of  $\tau_{\text{max}}$ , which characterizes the time range over which the nonexponential echo decay extends, is in agreement with the simulated one, assuming  $D = 5 \times 10^{-12}$  m<sup>2</sup>/s (Figs. 2 and 3). It should also be noted that the  $T_2^{\text{qe}}$  values obtained from the exponential part of the echo decay of experiment and simulation, respectively, agree very well. Hence lateral diffusion of the phospholipids along the curved membrane is indeed the dominating  $T_2^{\text{qe}}$  relaxation mechanism in spherical supported membranes.

It is interesting to compare this result (in particular the nonexponential echo decay) with the behavior observed

TABLE I. Results of the linear fitting of the first few points of the plot of  $1/T_2^{\text{CPMG}}$  vs  $\tau^2$  (cf. Fig. 5) for POPC vesicles of 640 nm diameter at a temperature of 10°C. The slope and the resulting lateral diffusion constant are given for linear fitting considering up to six data points at short time.

Temperature	$M_2$ (s <sup>-2</sup> )	Number of points	Slope ( $10^{11}$ s <sup>-3</sup> )	$D$ ( $10^{-12}$ m <sup>2</sup> /s)
10°C	7.7±0.6	3	2.7±1.9	1.8±1.3
		4	3.5±1.1	2.3±0.8
		5	2.9±0.7	1.9±0.6
		6	3.1±0.5	2.1±0.5
30°C	5.5±0.5	2	6.1±3.6	5.7±3.5
		3	4.3±1.6	4.0±1.3
		4	4.3±1.0	4.0±0.9
		5	3.9±0.7	3.6±0.9

and calculated for the case of  $T_2^{\text{qc}}$  relaxation due to mutual exchange for pairs of spin = 1 nuclei. Under conditions of intermediate exchange frequencies between the two sites and at sufficient short  $\tau$ , the echo decay exhibits a similar  $\exp(-\tau^3)$  dependence as reported above for lateral diffusion [30]. This is not surprising since both results are related to the well-known formula obtained for self-diffusion in liquids [31].

We want now to compare our values for the lateral diffusion coefficient  $D^{\text{CPMG}}$  of the phospholipids with those obtained by other methods. Our results agree with those obtained by the FRAP technique [1] for *N*-(7-nitro-2,1,3-benzoxadiazol-4-yl)-palmitoyl-oleoyl-phosphatidylethanolamine diffusion in POPC multilayers at similar temperatures and with those measured by pulsed-field-gradient NMR in POPC membranes [7]. The  $D$  values obtained by these methods are listed in Table II. The increase of  $D$  with temperature as measured by our CPMG method is in agreement with the "free volume model" suggested for the lateral diffusion in phospholipid bilayers [1,4].

Moreover, there is good agreement (at low temperature) with FRAP data obtained for the lateral diffusion of di-oleoyl-phosphatidylcholine (DOPC) [3], which resembles POPC but has two *cis*-unsaturated acyl chains. At higher temperature (45°C),  $D^{\text{FRAP}}$  for DOPC is approximately 30% higher than our value for POPC at 50°C. A possible reason for this faster diffusion of DOPC is a higher number of defects (free volumes) in the bilayer due to the *cis* double bond in both chains of DOPC. Another lipid mixture which can be expected to exhibit lateral diffusion properties similar to those of POPC is egg yolk lecithin (EYL). Its diffusion has been studied in lipid multilayers by FRAP [2] and in sonicated vesicles by analyzing the proton NMR line shape at different viscosities of the surrounding water [6]. Both methods provide  $D$  values which fit neatly into the temperature dependence which we measured for  $D^{\text{CPMG}}$  of POPC (cf. Table II).

Bimolecular reaction techniques were applied for the study of diffusion in EYL multilayers [4] by measuring the excimer formation of pyrene-labeled lecithin. This method gives  $D^{\text{exc}} = 1.3 \times 10^{-11} \text{ m}^2/\text{s}$  (30°C) and  $2.6 \times 10^{-11} \text{ m}^2/\text{s}$  (50°C). Hence  $D^{\text{exc}}$  indicates nearly one order of magnitude faster lateral diffusion than measured

by our method and by those listed in Table II. A similarly high lateral diffusion constant was measured recently in oriented multilayers of di-palmitoyl-phosphatidylcholine (DPPC) at 30°C ( $D^{\text{QENS}} = 1.4 \times 10^{-11} \text{ m}^2/\text{s}$ ) using QENS [9]. At 30°C DPPC is in the  $L'_\beta$  phase and all long-range lateral diffusion is essentially frozen [according to FRAP and pulsed-field-gradient (PFG) results]. Hence the QENS results presented by Tabony and Perly cannot be attributed to such processes but rather reflect the much faster local diffusion of the lipids. The reason for this is that in the momentum transfer range ( $q_{\text{min}}, q_{\text{max}}$ ) over which the above QENS experiment was performed, long-range lateral diffusion can be observed only at highest possible energy resolution  $\Delta E$ . Fitting high  $\Delta E$  and lower  $\Delta E$  data to one motional model (as done in [9]) then yields diffusion values which are dominated by local processes. Among these are confined diffusion (e.g., the back and forth jumps of a lipid molecule between two neighboring sites in the lattice) as well as intramolecular high-frequency motions like librational motion of the chains and segmental rotational jumps that will contribute to the QENS measurement.

Very recently, we did a QENS study on oriented DPPC multilayers using the same instruments as used by [9], but considered in the data analysis that only the measurements at highest-energy resolution (corresponding to effective lengths up to 30 Å) contain significant information about the lateral diffusion [10]. We obtained  $D = 9.7 \times 10^{-12} \text{ m}^2/\text{s}$  at 60°C which is about two orders of magnitude lower than the value suggested by [9] and thus fits well to the high-temperature values of our CPMG measurements and of the other methods as listed in Table II. The latter methods sample the average of a large sum of single lateral diffusion jumps over distances very large compared to the QENS length scale. The longest distances (in the  $\mu\text{m}$  range) are covered by FRAP and by pulsed-field-gradient NMR while the characteristic length scale of our CPMG method is significantly shorter (up to 100 nm). Despite these different length scales, these methods provide similar results which indicates that each method with a length scale sufficiently above that of a few lipid diameters is appropriate for a measurement of the lateral diffusion constant.

We want to refrain here from discussing the reasons

TABLE II. Comparison of the lateral diffusion coefficients  $D$  obtained for lipid multilayers at various temperatures by our CPMG technique ( $D^{\text{CPMG}}$ ), by the FRAP ( $D^{\text{FRAP}}$ ) technique (taken from [1]) for POPC, DOPC (taken from [3]), egg lecithin (EYL, taken from [2]), by the pulsed-field-gradient ( $D^{\text{PFG}}$ ) technique [taken from [7] and from [8](\*)], and by analysis of the proton NMR line shape ( $D^{\text{NMR}}$ ) of sonicated vesicles (taken from [6]).

Temperature (°C)	$D^{\text{CPMG}}$	$D^{\text{FRAP}}$	$D^{\text{FRAP}}$ ( $10^{-12} \text{ m}^2/\text{s}$ )		$D^{\text{PFG}}$	$D^{\text{NMR}}$
	POPC	POPC	DOPC	EYL	POPC	EYL
10	2.1±0.7		2.5			
15		2.8±0.3		2.8		
30	4.0±0.8	5.0±0.6			6.0±2*	4.0
35					6.0±2	
45		8.4±1.0	10.5			
50	7.0±1.0					

why excimer methods give similarly high  $D$  values than QENS. The presence of pyrene-labeled molecules at a concentration high compared to the label fraction used for fluorescence and ESR might cause inhomogeneities in the membrane (e.g., defect "grain" boundaries) and thus change the state of the system surrounding the pyrene label.

### CONCLUSIONS

We have presented an alternative method for measuring the lateral diffusion of the phospholipids in curved lipid membranes and found the results to be in excellent agreement with those obtained by FRAP and pulsed-

field-gradient methods on planar membranes. The temperature dependence of our data is in accordance with the "free volume" model of lateral diffusion. The significantly shorter characteristic length scale of our method and its independence of bulky labels makes it potentially useful for the study of demixing and domain formation processes in binary lipid mixtures. Such experiments on the phase disconnectivity in the two phase coexistence region of (nonideal) binary lipid mixtures are currently under way in our laboratory.

### ACKNOWLEDGMENTS

This work was supported by the SFB 266 (Project D-9) and by the BMFT.

\*Author to whom correspondence should be addressed.  
Electronic address: Thomas.Bayerl@bl.physik.tu-muenchen.de

- [1] W. L. C. Vaz, R. M. Clegg, and D. Hallmann, *Biochemistry* **24**, 781 (1985).
- [2] J. L. R. Rubenstein, B. A. Smith, and H. M. McConnell, *Proc. Natl. Acad. Sci. USA* **76**, 15 (1979).
- [3] R. Merkel, E. Sackmann, and E. Evans, *J. Phys. (Paris)* **50**, 1535 (1989).
- [4] H. J. Galla, W. Hartmann, U. Theilen, and E. Sackmann, *J. Membrane Biol.* **48**, 215 (1979).
- [5] P. F. Devaux and H. M. McConnell, *J. Am. Chem. Soc.* **94**, 4475 (1972).
- [6] M. Bloom, E. E. Burnell, A. L. MacKay, C. P. Nicol, M. I. Valic, and G. Weeks, *Biochemistry* **17**, 5750 (1978).
- [7] G. Lindblom, L. B.-A. Johansson, and G. Arvidson, *Biochemistry* **20**, 2204 (1981).
- [8] A.-L. Kuo and C. G. Wade, *Biochemistry* **18**, 2300 (1979).
- [9] J. Tabony and B. Perly, *Biophys. Biochim. Acta* **1063**, 67 (1990).
- [10] S. König, W. Pfeiffer, T. M. Bayerl, D. Richter, and E. Sackmann, *J. Phys. (Paris) II* **2**, 1598 (1992).
- [11] W. L. C. Vaz and P. F. Almeida, *Biophys. J.* **60**, 1553 (1991).
- [12] M. Bloom and E. Sternin, *Biochemistry* **26**, 2101 (1987).
- [13] J. Seelig and A. Seelig, *Quart. Rev. Biophys.* **13**, 19 (1980).
- [14] J. S. Blicharski, *Can. J. Phys.* **64**, 733 (1986).
- [15] T. M. Bayerl and M. Bloom, *Biophys. J.* **58**, 357 (1990).
- [16] C. Dolainsky, T. Köchy, C. Naumann, T. Brumm, S. J. Johnson, and T. M. Bayerl, in *The Structure and Conformation of Amphiphilic Membranes*, edited by R. Lipowsky, D. Richter, and K. Kremer, Springer Proceedings in Physics Vol. 66 (Springer-Verlag, Berlin, 1992), p. 34.
- [17] C. Dolainsky, A. Möps, and T. M. Bayerl, *J. Chem. Phys.* (to be published).
- [18] T. Brumm, A. Möps, C. Dolainsky, S. Brückner, and T. M. Bayerl, *Biophys. J.* **61**, 1018 (1992).
- [19] M. Rance and A. Byrd, *J. Magn. Reson.* **52**, 221 (1983).
- [20] E. M. Sternin, M. Bloom, and A. L. MacKay, *J. Magn. Reson.* **55**, 274 (1983).
- [21] S. T. Milner and S. A. Safran, *Phys. Rev. A* **36**, 4371 (1987).
- [22] F. Nezil, C. Morrison, K. P. Whittall, and M. Bloom, *J. Magn. Reson.* **93**, 279 (1991).
- [23] M. Bloom, C. Morrison, E. Sternin, and J. L. Thewalt, in *Pulsed Magnetic Resonance: NMR, ESR and Optics—a recognition of E. L. Hahn*, edited by D. M. S. Bagguley (Clarendon, Oxford, 1992).
- [24] A. Abragam, *Principles of Nuclear Magnetism* (Oxford University Press, London, 1961).
- [25] H. Y. Carr and E. M. Purcell, *Phys. Rev.* **94**, 630 (1954).
- [26] S. Meiboom and D. Gill, *Rev. Sci. Instrum.* **29**, 688 (1958).
- [27] M. Bloom and E. Evans, in *Biologically Inspired Physics*, edited by L. Peliti (Plenum, New York, 1991).
- [28] P. I. Watnick, P. Dea, and S. Chan, *Proc. Natl. Acad. Sci. USA* **87**, 2082 (1990).
- [29] J. Stohrer, G. Gröbner, D. Reimer, K. Weisz, C. Mayer, and G. Kothe, *J. Chem. Phys.* **95**, 672 (1991).
- [30] K. Müller, R. Poupko, and Z. Luz., *J. Magn. Reson.* **90**, 19 (1991).
- [31] H. C. Torrey, *Phys. Rev.* **104**, 563 (1956).